CrossMark

Prediction of collective actions using deep neural network and species competition model on social media

Wei Yang[1] · Xiao Liu[2] · Jin Liu[3,4,5] · Xiaohui Cui[1]

Abstract

Collective actions that can affect government management and public security (e.g., mass demonstrations), usually undergo long term development and originate from small and uncertain social media activities. Thus, researchers try to identify a collective action from various aspects such as changes in communication patterns, emerging keywords, and social emotions. Many studies aim to predict whether regular social media activities can evolve into collective actions, but the accuracy of these predictions is far from desirable. To address such a problem, we propose a framework named PFDNN which can predict the occurrence probability of collective actions every single day in the next month, so as to provide a reference for early decision-making. The framework consists of two parts: collective emotional contagion prediction and deep neural network with fully-connected layers (DNN) prediction. First, we implement the emotional contagion prediction based on species competition model to forecast user's emotional state. Second, we model the DNN prediction as a binary classification problem that can be implemented using a DNN discriminator based on emotional contagion prediction. The DNN discriminator considers early premonitions based on the number of tweets, the embedded emotions and the number of violence-related words in the tweets during a specific timeframe, and automatically labels the early premonitions according to the number of reports published in the mainstream media. For evaluation purpose, we analyze the topics related to the "Arab Spring" from over 300,000 social media entries using TensorFlow. The results demonstrate that our prediction framework performs better than other representative methods.

Keywords Collective action · Emotional prediction · Automatic label · Deep neural network · Early premonitions

1 Introduction

A social media is composed of actors (e.g., individuals or organizations), dyadic ties, and social interactions among actors [1–6]. The development of information technologies and

✉ Xiaohui Cui
  xcui@whu.edu.cn

  Extended author information available on the last page of the article

the Internet has widely boosted the use of social media or social network [7–10]. According to an eMarketer report, there are 1.82 billion worldwide users of social media tools such as Facebook Messenger and WeChat by 2017, with an average growth rate of 15.5% per year [11]. Furthermore, social media plays an important role in our daily life for information dissemination, and it makes much more convenient for information exchange among actors including ordinary people, businesses, and activists. However, social media can also produce negative effects to the society. In some cases, it may become the source for collective actions such as terrorism and social uprising including the notorious "Arab Spring" as an example of the latter [12]. Collective actions, especially those during social conflicts, might severely affect economic development, social order, and public safety. It is usually organized by a group of people aiming to enhance their social status and achieve a common objective [13]. Social media provides a channel that allows those people to spread messages for collective actions. For instance, in 2011, the massive collective action called "Occupy Wall Street" started in New York. Within a month, its scale jumped from tens of local people to tens of thousands of people from over 950 cities in North America, Asia, Europe, and Oceania. This event demonstrated that social media can provide a much faster means to disseminate information than traditional media. In fact, the hashtag "#OccupyWallStreet" appeared on Twitter only one night before the uprising on September 16th, 2011. Afterwards, during the first two weeks of this collective action, more than 10,000 videos on this topic were uploaded to YouTube, which makes it the biggest video sharing event related to a single activity in the world [9–14]. Qualitative analyses have revealed that more than 75% of the protests are planned, organized, and announced in advance, and individuals are very likely to express themselves about these topics on social media [15–17]. Therefore, predicting the occurrence of collective actions by analyzing entries on social media is possible and of great significance.

Collective actions usually begin a long time before the occurrence of major events, and some early premonitions can distinguish them from regular activities. For this study, we consider three features to describe early premonitions related to a topic: the numbers of tweets, the number of violence-related words, and the negative emotion embedded in the tweets. Apparently, regular events about social problems can evolve into a collective action if they attract the attention from the public and the number of tweets can represent the most intuitive parameter to measure the public's attention. Meanwhile, violence-related words are more frequently used in the context of a collective action than in regular social media activities. In addition, we employ negative emotion as a supporting feature for our analysis when there are no sufficient violence-related words. If the future emotion were to be positive, we would conclude that the regular activity will not evolve into a collective action. At an early stage, there might be only a slight difference between a potential collective action and a regular social activity. To distinguish the prelude of a collective action (quantified by the features of related tweets) from a regular social activity, we analyze the combination of features during a timeframe to generate what we called early premonitions. By using early premonitions, we can predict whether a regular social activity can evolve into a collective action and estimate its date of occurrence. Implemented using a deep neural network (DNN) [18–21], we model the prediction framework as a binary classification problem where regular activities and collective actions are the two classes. The framework retrieves early premonitions from social media data and uses mainstream media data to verify the occurrence of collective

actions. Specifically, we use mainstream media data to label early premonitions during the training process of the DNN.

The main contributions of this study are summarized as follows:

1) **Prediction framework**. We propose a framework to predict the occurrence and the date for collective actions based on social and mainstream media data.
2) **Discriminator**. We model the prediction of collective actions as a binary classification problem and solve with a DNN discriminator. The training data are automatically labeled based on the number of reports published in the mainstream media.
3) **Early premonitions**. We consider three features of tweets during a timeframe. These features formalize and quantify the early premonitions for collective actions which are used as the inputs for the DNN training set.
4) **Emotional contagion prediction**. We proposes a prediction model based on the species competition model and the epidemic model that can predict collective emotional contagion for the dynamic development of a specific topic event before the decay period on social media.

The remainder of this paper is organized as follows. Section 2 overviews the framework and proposes the assumptions used in this study. Section 3 describes the collective emotional contagion and species competition model. Section 4 describes the early premonitions and automatic labeling for DNN prediction. Section 5 presents the technical details of DNN prediction. Section 6 demonstrates the performance evaluation results of the prediction framework. Section 7 presents the related work. Finally, Section 8 concludes this paper.

2 Framework overview and assumptions

The overview of the framework is shown in Figure 1 and with more details presented in Figure 4. The framework mainly consists of two steps: if it predicts positive emotion in the future, we would consider that the regular social media activity will not evolve into a collective
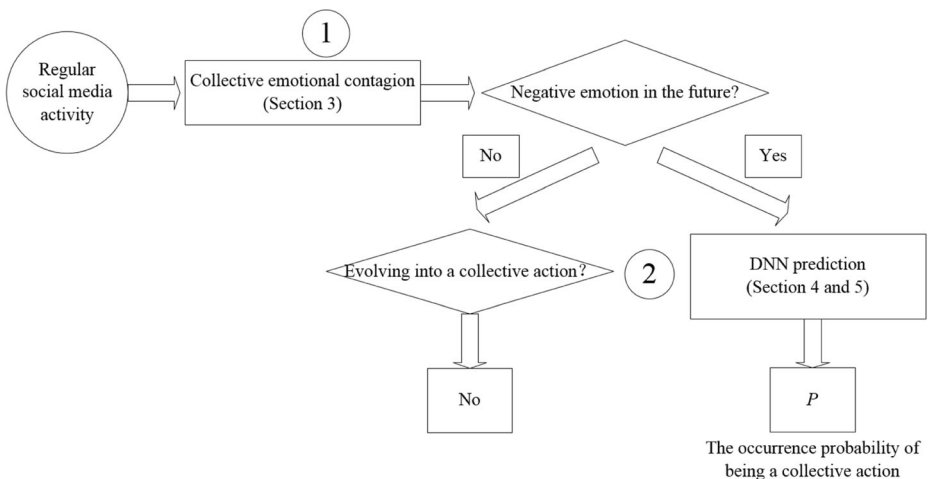

Figure 1 Framework Overview

action; if it predicts negative emotion in the future, we would use the DNN (Deep Neural Network with fully-connected layers) prediction to forecast the occurrence probability of the regular social media activity evolving into a collective action.

Here, we present some assumptions used in this paper:

1. The total number of users on the social media remains at a constant value N.
2. There are four groups of users on the social media: users who hold a positive emotion (Group I_p), the users who hold a negative emotion (Group I_n), the users who were members of I_p or I_n in the past (Group I_r), but no longer pay attention to the event, and the users who haven't been susceptible to emotional contagion related to the relevant event (Group I_s). The research also assumes that $I_{pn} = I_p \cup I_n$. At the initial stage we just focus on three groups: I_p, I_n, I_s. The number of users in I_p, I_n, I_r, I_s at time t are denoted as $x_p(t), x_n(t), s(t), r(t)$ respectively.
3. $\lambda_i (i = 1,2)$ represents the growth rate of the users' followers who start to discuss the specific topic event in group I_p or I_n
4. The immunization proportion is denoted as u and is considered to be a constant. Several users in I_{pn} may become members of I_r at every time step and this proportion is denoted as u.
5. Once the users are aware of the relevant event under study, they can just keep one certain emotion, either positive or negative.
6. There are interaction effects between I_p and I_n during the process of information dissemination.

3 Collective emotional contagion

The Collective Emotional Contagion Model (CECM) focuses on predicting the future emotion of the regular social media activities. The whole scenario of collective emotional contagion is illustrated in Figure 2. We assume there are two kinds of collective emotions: positive and negative. The prediction model for collective emotional contagion comprises two stages. In the first phase, some messages are propagated to a few opinion leaders who have many followers and can propagate message widely and rapidly on social media. Theses opinion leaders express their opinions and several followers share these messages. Because of the influence of the opinion leaders, the messages can be spread quickly and discussed intensively among their followers on social media. However, most followers may not understand or know the facts of the messages clearly during the initial period, they are largely influenced by the opinion leaders' opinions and emotions. After some time of information dissemination, users on the social media are evolved into three groups, I_p, I_n and I_s, at time point t_1, as shown in Figure 2. The followers' emotion could now be either positive or negative, even though they may still not know or understand the messages. In this phase, the scales of I_p and I_n gradually increases, while I_s is observed to be diminishing.

In the second phase, a new group I_r appears and increases gradually along the timeline of the message. It means that some users in I_p or I_n become members of I_r. The information dissemination of the users' emotions can is like the spread of an epidemic. The users in the group I_r are the immune individuals and users in I_p or I_n are patients. There are mutual transformations and exchanges within the four groups. For example, some followers in I_p and I_n can transfer into members in I_r, and some followers in I_s can transfer into members in I_p or I_n. Similarly, with the development of the relevant event, transformations and exchanges among
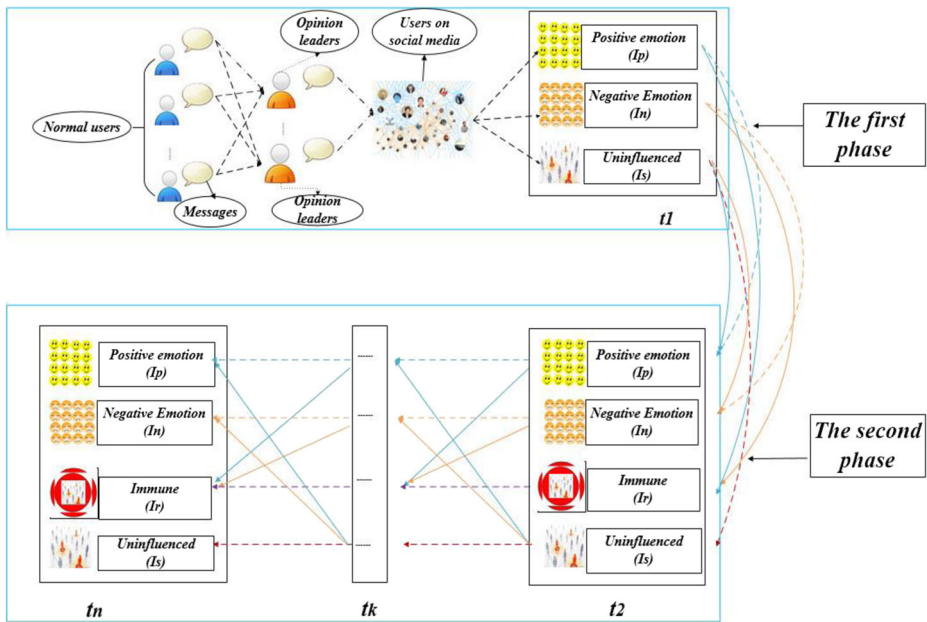
Figure 2 Overview of scenario for information dissemination on social media

the four groups will continue until the event ended. Another important reason why this study divides the prediction framework into two phases is that sometimes new facts may be unfolded during the development of the specific event, which may affect the emotional contagion.

To predict the future emotional state, CECM is proposed in this paper based on the species competition [22–26]. To apply the model to predict collective emotion, the competition relation is represented by the influence between the two groups, I_p and I_n, as an analogy to two species in the species competition model. In addition, the users in I_s are described by using an analogy to the living resource in the species competition model explained as follows.

3.1 Species competition model

If there are two or more kinds of species in nature, there may be mutual competition, interdependence or predator-prey relations among them [22–26]. This section focuses on the competition relation. If the resources that support their lives are limited, the species may compete with each other [27–30]. Eventually, weaker species may die out and the number of stronger species will live. Here, the species competition model is formally presented.

Firstly, let us analyze a situation in which there is no competition among species. If two kinds of species A and B live in their independent habitats, the evolution of the number of the species follows logistic distribution [28]. The number of species A and B are denoted as $x_1(t)$, $x_2(t)$ respectively at a point of time t. The initial growth rates are r_1 and r_2 respectively, while N_1 and N_2 are the maximum number of the species that their respective habitats can support. As increase in the number of species A may lead to the decline of the growth rate. This relation is described with a linear function $r(x_1) = r_1 - s * x_1$ $(r_1 > 0, \ s > 0)$ where $r_1 \ (N_1) = 0$, $s = r_1/N_1$. s is used to describe the decay rate of the

growth rate $r(x_1)$. In this paper, we build an ordinary differential equation for the growth rate as in Eq. (1).

$$\frac{dx_1}{dt} = r(x_1)*x_1$$
$$\frac{dx_1}{dt} = (r_1-s*x_1)*x_1$$
$$\frac{dx_1}{dt} == r_1*x_1*(1-), x_1(0) = x_{10}$$

(1)

where $r_1 x_1$ reflects the growth trend of the number and $(1-x_1/N_1)$ reflects the block effect of lacking resource.

Similarly, the ordinary differential equation of x_2 for species B is

$$\frac{dx_2}{dt} = r_2*x_2*(1-), x_2(0) = x_{20}$$

(2)

Furthermore, we investigate the competition relation in the same habitat where A and B are competing for the same resources. To represent the competition from B to A, $(1-x_1/N_1)$ is modified to $(1-x_1/N_1-\sigma_1 x_2/N_2)$ so as to include the fact that an individual B can consume σ_1 times the number of resources than an individual A. Thus, the ordinary differential equation of x_1 is shown in Formula (3)

$$\frac{dx_1}{dt} = r_1*x_1*\left(1-\frac{x_1}{N_1}-\sigma_1\frac{x_2}{N_2}\right), x_1(0) = x_{10}$$

(3)

Similarly, B also affects the increase of A and the corresponding ordinary differential equation is depicted in Formula (4)

$$\frac{dx_2}{dt} = r_2*x_2*\left(1-\sigma_2\frac{x_1}{N_1}-\frac{x_2}{N_2}\right), x_2(0) = x_{20}$$

(4)

where σ_2 denotes that an individual A can consume σ_2 times living resources than an individual B.

In species competition model, σ_1 and σ_2 are the two critical variables that represent the competitiveness in resources. If $\sigma_1>1$, the competitiveness of B is higher than that of A, vice versa when $\sigma_2 >1$.

3.1.1 Collective emotional contagion model

The study in [31] found that the collective opinion of the steady state may deviate to the positive or negative direction because of the initial bias of the leaders' opinions. Meanwhile, opinion leaders usually have many followers on social media, which may affect the collective opinion in the process of information dissemination. However, with the wide spread of information, the opinion leaders' influence may decline because the public opinions may play a more important role in emotional contagion.

The collective emotional contagion model considers both the positive and negative opinions. During the dissemination process, the two opinions can affect each other. Using the analogy of species in nature, the users who hold different opinions can be regarded as different species. This research tries to simulate the emotional contagion process using the species

competition model. In the model, the number of I_p, I_n, I_r, I_s are $i_p(t)$, $i_n(t)$, $r(t)$ and $s(t)$ respectively at time t, and $i(t) = i_p(t) + i_n(t)$.

Note that here the precondition is that the event has happened for a period of time. To simplify the description, the users who have discussed the specific event and held the positive emotion are defined as group I_{p0}. The length of I_{p0} is m, which means the number of the users who have expressed their emotion. Similarly, the users who have held the negative emotion are defined as group I_{n0}. For I_p, r_1 that represents initial growth rates is substituted by λ_1 quantized with the users' followers in group I_{p0}. Similarly, r_2 is substituted by λ_2 quantized with the users' followers in group I_{n0}. Additionally, the parameter σ_1 reflects the competitiveness of I_n which is measured with the users' reliability in group I_{n0}. For example, on the social media, the followers forward or like the posts only if they are more persuasive and credible, and the number of followers who can affect the speed of information dissemination. So the reliability can be quantized based on the reliability of users' opinion measured by the number of forwards and likes of the posts, and the number of followers for every user in I_{n0}. Thus, σ_1 is defined as in formula (5) where α and β represent the weights of the users' reliability and the number of followers respectively, $n_{i,nfo}$ represents the number of forwarded $user_i$'s posts in I_{n0}, $n_{i,nlike}$ represents the number of $user_i$'s liked posts in I_{n0}, $n_{j,pfo}$ represents the number of forwarded $user_j$'s posts in I_{p0}, $n_{j,plike}$ represents the number of $user_j$'s liked posts in I_{p0}, $\lambda_{i,nfan}$ represents the number of $user_{is}$'s followers in I_{n0}, and $\lambda_{j,pfan}$ represents the number of $user_j$'s followers in I_{p0}.

$$\sigma_1 = \alpha\sum_i\left(n_{i,nfo} + n_{i,nlike}\right) + \beta\sum_i\lambda_{i,nfan} \tag{5}$$

Similarly,

$$\sigma_2 = \alpha\sum_j\left(n_{j,pfo} + n_{j,plike}\right) + \beta\sum_j\lambda_{j,pfan} \tag{6}$$

3.2 The contagion process

With the development of the event, some users will no long care about the relevant messages, and hence users in groups I_p and I_n may be transferred into I_r. That is, the proportion of each emotional group that may be reduced is the immunization proportion u at each time step $\triangle t$ according to the assumption 4. Thus, the emotional contagion process can be improved to the Formula (7) based on Formula (2) and Formula (4).

$$\begin{cases} \dfrac{dx_p}{dt} = \lambda_1 *x_p *\left(1 - \dfrac{x_p}{N_1} - \sigma_1\dfrac{x_n}{N_2} - u\right) \\ \dfrac{dx_n}{dt} = \lambda_2 *x_n *\left(1 - \dfrac{x_n}{N_2} - \sigma_2\dfrac{x_p}{N_1} - u\right) \\ x_p, x_n \geq 0 \end{cases} \tag{7}$$

Referring to the species competition model, if $\sigma_1 > 1$, the ability of users in I_n to influence users from I_s who hold the positive opinion at first into I_n is higher than that of users in I_p. In such a situation, the users in I_s may transfer to negative opinion. Similarly for the situation when $\sigma_2 > 1$.

3.2.1 Analysis of stability

This section focuses on analyzing the stability of CECM which can predict the final stable emotional state of information dissemination before the decay period. Stability can be

described by the trends of x_p, x_n. However, the analytic equation of Formula (7) is very difficult to be solved. Luckily, x_p, x_n at each time step can be estimated using the Runge-Kutta algorithm which is used to solve ordinary differential equations based on the iterative algorithm. Meanwhile, the last states of x_p, x_n can be described with equilibrium points. We set $f(x_p, x_n) \equiv dx_p/d_t$, $g(x_p, x_n) \equiv dx_n/d_t$, and $f(x_p, x_n) = 0, g(x_p, x_n) = 0$ to get equilibrium points.

$$\begin{cases} f(x_p, x_n) \equiv \lambda_1 * x_p * \left(1 - u - \dfrac{x_p}{N_1} - \sigma_1 \dfrac{x_n}{N_2}\right) = 0 \\ g(x_p, x_n) \equiv \lambda_2 * x_n * \left(1 - u - \dfrac{x_n}{N_2} - \sigma_2 \dfrac{x_p}{N_1}\right) = 0 \\ x_p, x_n \geq 0 \end{cases} \tag{8}$$

After solving the equations, we get four equilibrium points, $P_1(N_1, 0)$, $P_2(N_2, 0), P_3(\frac{N_1(1-\sigma_1)(1-u)}{1-\sigma_1\sigma_2}, \frac{N_2(1-\sigma_2)(1-u)}{1-\sigma_1\sigma_2})$, $P_4(0,0)$. Clearly, we can see that the final stable values of x_p, x_n only depend on the values of u, N_1, N_2, σ_1 and σ_2.

This research analyzes the stability of the equilibrium points based on the stability theory of ordinary differential equations [24]. According to the method that justifies the stability, we give the coefficient matrix (A) of formula (8) and two indicators (p,q) that are used to justify the stability of the equilibrium points.

$$A = \begin{bmatrix} f_{x_p} & f_{x_n} \\ g_{x_p} & g_{x_n} \end{bmatrix}$$

$$= \begin{bmatrix} \lambda_1\left(1 - \dfrac{2x_p}{N_1} - \dfrac{\sigma_1 x_n}{N_2} - u\right) & \dfrac{-\lambda_1 p \sigma_1 x_p}{N_2} \\ \dfrac{-\lambda_2 p \sigma_2 x_n}{N_1} & \lambda_2\left(1 - \dfrac{2x_n}{N_2} - \dfrac{\sigma_2 x_p}{N_1} - u\right) \end{bmatrix}$$

$$p = -\left(f_{x_p} + g_{x_n}\right)\Big|_{p_i}, i = 1,2,3,4$$

$$q = \det A\big|_{p_i}, i = 1,2,3,4$$

If the equilibrium points are stable, $p > 0$ and $q > 0$ according to stability theory. The requirements are described in Table 1. Additionally, our experiments revealed that λ_1 and λ_2 should be larger than a threshold depending on u, σ_1 and σ_2.

Actually, the emotional trend in the stable state, which is affected by p and q, can be analyzed based on the equilibrium points as shown in Table 1. For the equilibrium points P_1 and P_2, the emotional trend depends on the maximum. For P_3, the emotional trend depends on $N_1(1-\sigma_1)(1-u)$ and $N_2(1-\sigma_2)(1-u)$. Thus, the proportion of the users with positive emotion and the proportion of the users with negative emotion are calculated using Formula (9) as follows:

$$P_{Ip} = \frac{\dfrac{N_1(1-\sigma_1)(1-u)}{1-\sigma_1\sigma_2}}{\dfrac{N_1(1-\sigma_1)(1-u)}{1-\sigma_1\sigma_2} + \dfrac{N_2(1-\sigma_2)(1-u)}{1-\sigma_1\sigma_2}} = \frac{N_1(1-\sigma_1)}{N_1(1-\sigma_1) + N_2(1-\sigma_2)} \quad P_{In} = 1 - P_{Ip}$$

$$= \frac{N_2(1-\sigma_2)}{N_1(1-\sigma_1) + N_2(1-\sigma_2)} \tag{9}$$

Table 1 Requirements of stability for the equilibrium points

equilibrium points	p	q	Requirements of stability
$P_1(N_1,0)$	$\lambda_1(u+1)- \lambda_2p(1\text{-}\sigma_2\text{-}u)$	$-\lambda_1\lambda_2*(1\text{-}\sigma_2\text{-}u\text{-}u^2)$	$\sigma_1<1\text{-}u,\ \sigma_2>1\text{-}u$
$P_2(0,N_2)$	$\lambda_2(u+1)- \lambda_1p(1\text{-}\sigma_1\text{-}u)$	$-\lambda_1\lambda_2*(1\text{-}\sigma_1\text{-}u\text{-}u^2)$	$\sigma_1>1\text{-}u,\ \sigma_2<1\text{-}u$
$P_3(\frac{N_1(1-\sigma_1)(1-u)}{1-\sigma_1\sigma_2}, \frac{N_2(1-\sigma_2)(1-u)}{1-\sigma_1\sigma_2})$	$\frac{(1-u)(\lambda_1(1-\sigma_1)+\lambda_2p(1-\sigma_2))}{1-\sigma_1\sigma_2}$	$\frac{\lambda_1\lambda_2(1-\sigma_1)(1-\sigma_2)(1-u)^2}{1-\sigma_1\sigma_2}$	$\sigma_1<1\text{-}u,\ \sigma_2<1\text{-}u$
$P_4(0,0)$	$-(\lambda_1+\lambda_2)(1-u)$	$\lambda_1\lambda_2(1-u)^2$	No stable

4 Early premonitions and automatic labeling

In this section, we describe the definition of early premonitions for collective actions and their automatic labeling which is the preprocessing for DNN prediction as will be introduced in section 5.

We define early premonitions based on the combination of three features observed over a period of time, including: signal S, violence-related words V, and emotion E. These features are extracted from social media, and early premonitions are represented as a time series, namely (S_i, V_i, E_i) represents the early premonition on day i. Each feature is defined as follows.

Signal S We define the signal as the number of tweets about a specific topic during a day which aims to reflect the attention from the public. In addition, we normalized S_i using (10) to obtain $S'_i = f(S_i)$.

$$f(x) = \frac{x - x_{min}}{x_{max} - x_{min}} \tag{10}$$

Violence-related words V Expressions such as "protest," "war crimes," "demonstration against," and "parade" suggest that a related event might result in a collective action involving some type of violence [32]. We define V_i as the average number of violence-related words in all the tweets about a specific topic during a day. To identify these words, we build a violence-related lexicon based on word embedding. First, we select a few violence-related words, such as protest, bomb, and march. Then, we use a skip-gram model to train the word embedding for the words in a corpus. We compute the cosine similarity given by Formula (12) between the words in the corpus and each of the selected violence-related words for word embedding. Next, we add the K candidate violence-related words most similar to each selected word to the lexicon, and remove the duplicates. To improve the lexicon quality, the candidate violence-related words are confirmed artificially by analyzing whether they have been frequently used in collective actions. Finally, the average number of violence-related words can be obtained by searching in tweets during a day. We also normalized V_i using Formula (11). The process for searching violence-related words in a tweet is described in **Process 1**.

Process 1. Lexicon and number of violence-related words per tweet
Input: Predefined violence-related words
Output: Violence-related lexicon W and number of violence-related words v per tweet
       1. Use skip-gram model to train word embedding for each word in the corpus
       2. For each word w_i in the corpus
3. compute the cosine similarity between w_i and each predefined violence-related word with word embedding
       4. For each predefined violence-related word
       5. select the K most similar candidate words as synonyms based on similarity
       6. remove duplicates among synonyms
       7. verify the obtained words artificially and generate lexicon W
       8. For each tweet in the dataset
       9. obtain the number of violence-related words based on lexicon W
       10. Return W and v

$$V'_i = f\left(\frac{\sum_{j=1}^n v_{ij}}{n_i}\right) = \frac{\sum_{j=1}^n v_{ij} - v_{min}}{n_i {}^* (v_{max} - v_{min})} \tag{11}$$

where v_{ij} denotes the average number of violence-related words for the j-th tweet on the i-th day, $\sum_{j=1}^n v_{ij}$ denotes the total number of these words on the i-th day, n_i denotes the number of tweets related to a topic on the i-th day, v_{min} denotes the minimum number of violence-related words found in tweets along the days, and v_{max} denotes its maximum.

$$Cosine\_similarity = \frac{\sum_{k=1}^m x_{1k} {}^* x_{2k}}{\sqrt{\sum_{k=1}^m x_{1k}{}^2} {}^* \sqrt{\sum_{k=1}^m x_{2k}{}^2}} \tag{12}$$

where x_1 and x_2 denote vectors with elements x_{1k} and x_{2k}, respectively, and *Cosine_similarity* is the cosine similarity between the two vectors.

Emotion E The emotion reflects the emotional content of tweets. We only consider negative emotion determined by analyzing the content of tweets using the tool TextBlob. This tool returns emotion values $E \in [-1, 1]$ where negative emotions belong to $(-1, 0)$ and $|E|$ represents the level of the emotion. For a given day i, we define emotion E_i as the average emotion of the tweets related to a topic. We find that collective actions show a tendency towards negative emotion. To obtain the normalized feature, we apply Formula (10) to the corresponding arguments as defined in Formula (13). This way, negative emotion is mapped to the interval $(0.5,1]$ and positive emotion to the interval $[0,0.5]$. Furthermore, the most positive emotion maps to 0, and the most negative emotion maps to 1.

$$E'_i = f\left(-\frac{\sum e_{ij}}{n_i}\right) = \frac{-\frac{\sum e_{ij}}{n_i} - e_{min}}{e_{max} - e_{min}} \tag{13}$$

where n_i denotes the number of the tweets related to a topic on the i-th day, e_{ij} denotes the emotion of the j-th tweet on the i-th day, $\frac{\sum e_{ij}}{n_i}$ denotes the average emotion of tweets on the i-th day, e_{min} denotes the minimum average emotion of tweets along the days, and e_{max} denotes its maximum counterpart.

Determining early premonitions and automatic labeling The features outlined above aim to establish the connection between early premonitions X_i (correspond to the inputs of the framework extracted from social media) and future condition Y_j (correspond to the outputs of the framework extracted from mainstream media and is automatically labeled). In our framework as shown in Figure 3, samples in a training set associated with early premonitions are labeled either with $Y_j = 1$ or 0. To obtain samples for the training set, we first confirm the value of Y_j and then build the corresponding early premonitions. Early premonitions are based on the features of tweets during k days, namely from day $j–k–m + 1$ to $j–m$, if the framework aims at predicting whether the collective action will occur or not m days later, i.e., on day j. For instance, if $m = 1$, the framework predicts whether the collective action will occur tomorrow.

To automatically label the early premonitions, we consider the occurrence date (i.e., day j) of the collective action based on the number of relevant news published on mainstream media,

and denote the corresponding signal as $S_{m,j}$ on day j. In [32], it is proposed a threshold $\theta' =$ 2.875 based on the number of relevant reports, where $\theta = g(S_{m,j}) > \theta'$ indicates the occurrence of a collective action (i.e., $Y_j = 1$), and g denotes a transformation function given by

$$\theta = g\left(S_{m,j}\right) = \frac{1}{3}\sum_{t=j-1}^{j+1}\frac{S_{m,t}}{\overline{S}'_{m,j}}$$

$$\overline{S}'_{m,j} = \frac{1}{90}\sum_{j=i-90}^{i-1}S_{m,i}$$

(14)

where $\overline{S}'_{m,j}$ represents the average times a topic has been mentioned in the last three months to stabilize the value.

For regular activity (i.e., $Y_j = 0$), we also obtain the corresponding early premonitions. Hence, for regular activity or a collective action to occur on day j, we formalize the corresponding early premonitions X_j considering signal S, violence-related words V, and emotion E as follows:
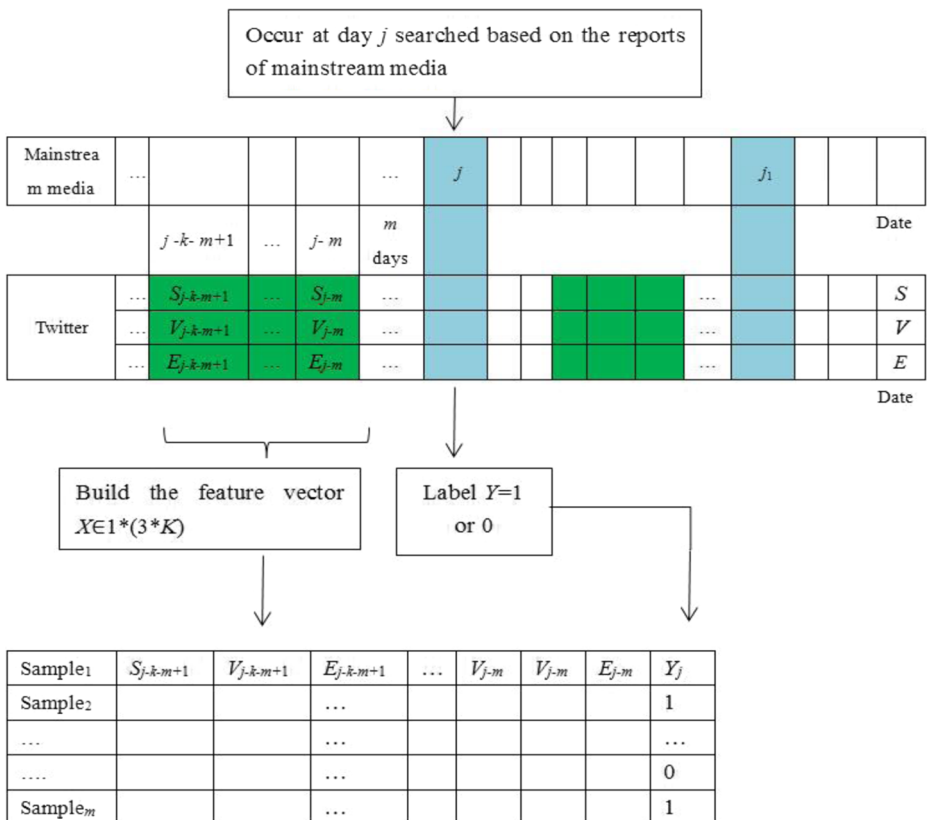
Figure 3 Prediction mechanism based on early premonitions of collective actions and automatic labeling from mainstream media

$$X_j = \left(X'_{j-k-m+1}, X'_{j-k-m+2}, \cdots X'_{j-m}\right), j = m+1, m+2, \ldots, n$$
$$= \left[\left(S_{j-k-m+1}, V_{j-k-m+1}, E_{j-m+1}\right), \left(S_{j-k-m+2}, V_{j-k-m+2}, E_{j-k-m+2}\right), \cdots, \left(S_{j-m}, V_{j-m}, E_{j-m}\right)\right]$$

$$(15)$$

where $X'_{j-k-m+1}$ denotes the transpose of matrix of $X_{j-k-m+1}$ and $X'_{j-k-m+1} = (S_{j-k-m+1}, V_{j-k-m+1}, E_{j-m+1}) \in R^{1*3}$ are the three features on day $j-m$.

5 DNN prediction

We implement the prediction framework using a DNN, and collect a large dataset of tweets by dates. The framework incorporates four stages: 1) Build the training set: extract the number of news published on mainstream media to obtain θ from Formula (14)(step①②in Figure 4); automatically label the training set by transforming θ to label $Y = 1$ or 0; extract the three features from social media(tweets) in the dataset to build the corresponding early premonitions (step③④in Figure 4); 2) Use Collective Emotional Contagion Model (CECM) to predict the future emotion of the regular social media activities (step⑤in Figure 4); 3) If the future
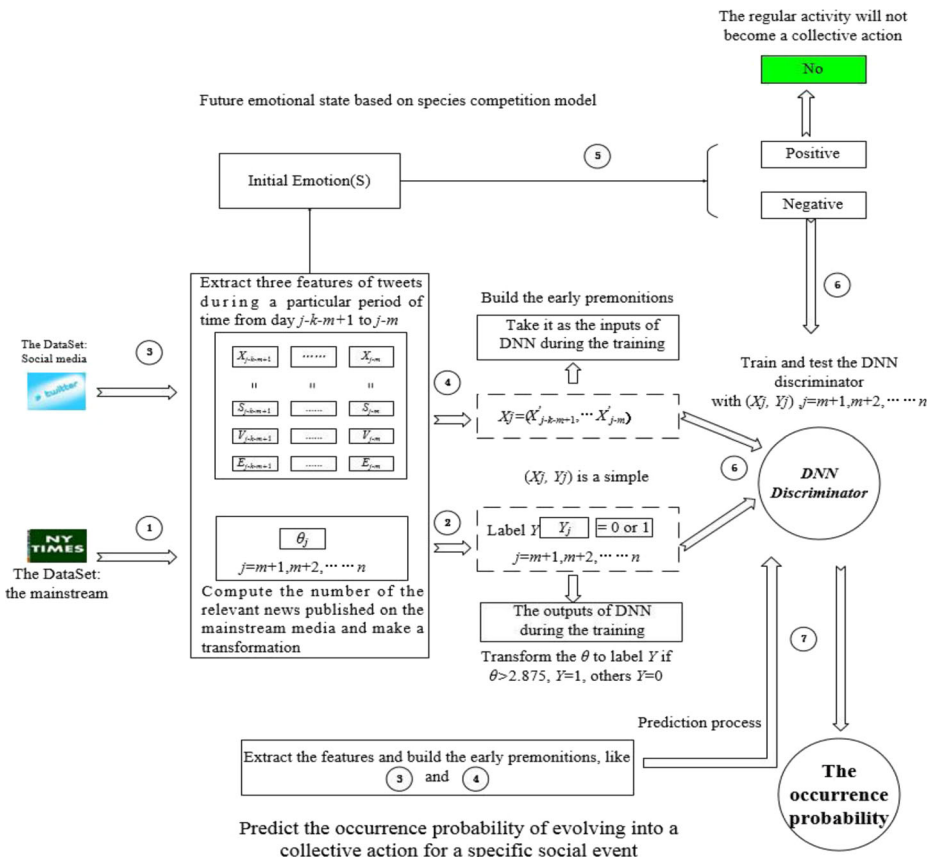

Figure 4   Prediction framework for collective actions

emotion is negative, train and test the DNN discriminator with early premonitions X_j as inputs and labels Y_j as outputs, namely pairs of samples (X_j, Y_j), $j = m + 1, m + 2, \ldots, n$ are used to train the DNN (step⑥in Figure 4); 4) Predict the occurrence probability of regular social media activity evolving into a collective action for a specific social event (step⑦in Figure 4). The DNN discriminator for the prediction framework is depicted in Figure 4.

5.1 DNN discriminator

We employ the DNN discriminator to determine whether a regular social media activity can evolve into a collective action on day j which is m days after our analysis. The main idea depends on analyzing early premonitions during the k days before the day of the prediction, namely on day j–m, and their relation to the occurrence probability of a collective action on day j by analyzing the relation between the inputs (i.e., early premonitions) and the outputs (i.e., whether a collective action occurs). As mentioned above, we train the DNN discriminator with samples (X_j, Y_j), $j = m + 1, m + 2, \ldots, n$.

For the training process, the inputs and outputs are X_j and Y_j, respectively. The predicted value for Y_j is denoted as $\overline{Y}_j$. The details of the discriminator structure are described as follows.

1) The activation function for the hidden layers is $tanh(z)$ as defined in Formula (16). Our experiments show that it performs better than other activation functions.

$$tanh(z) = \frac{sinh(z)}{cosh(z)} = \frac{e^{z} - e^{-z}}{e^{z} + e^{-z}} \tag{16}$$

The output for the hidden layers is defined as a^{l+1} based on the activation function:

$$
\begin{aligned}
a^{l+1} &= tanh\left(z^l\right) \\
&= tanh\left(\left(w^{l*}a^l\right) + b^l\right) \\
&= \frac{e^{\left(w^l*a^l\right)+b^l} - e^{-\left(w^l*a^l\right)+b^l}}{e^{\left(w^l*a^l\right)+b^l} + e^{-\left(w^l*a^l\right)+b^l}}
\end{aligned}
\tag{17}
$$

where $w^l \in R^{k*m}$ is the weight vector of the l-th layer, $a^l \in R^{m*n}$ represents the nodes of the l-th layer, $b^l \in R^{1*n}$ is the bias vector of the l-th layer, $(w^l*a^l) + b^l$ denotes the inputs of the $(l + 1)$-th layer, and $a^{l+1} \in R^{k*n}$ represents the outputs of the $(l + 1)$-th layer.

2) Given that it is a probability classification problem, the outputs for the final layer, given by a score vector per category, are determined by Formula (18) based on the activation function. Namely that $\overline{Y}$ can show the occurrence probability of collective actions. The category with the highest score is regarded as the prediction.

$$\overline{Y} = f(z) = \frac{e^{\left(w^l*a^l\right)+b^l}}{\sum_{l=1}^{2} e^{\left(w^l*a^l\right)+b^l}} \tag{18}$$

where $\overline{Y} \in R^{1*2}$ is the l-th node of the output layer which ranges from 0 to 1 and represents the probability of the sample belonging to one of the 2 classes.

3)   The optimization objective of the DNN is based on the mean squared error and L2 regularization to prevent overfitting, given by Formula (19)

$$C = \frac{1}{n}\sum_{k=1}^{n}\sum_{i=1}^{2}\left(Y_{k,i}-\overline{Y}_{k,i}\right)^2 + \lambda^*\sqrt{\sum_i\sum_j w_{ij}^2} \tag{19}$$

Where n represents the number of the samples, $Y_{k,i} \in \{0, 1\}$ represents the label for the sample, $\overline{Y}_{k,i}$ represents the prediction probability of the k-th sample belonging to the i-th class, w_{ij} represents the weight of the j-th node at the i-th layer of the network, and λ represents the weight for the L2 regularization.

6 Experiments and analysis

As the prediction framework mainly consists of two parts: the collective emotional contagion based on species competition model and the DNN prediction process, we evaluate the performances of the two parts respectively. First, we evaluate the performance of CECM. The experiments mainly evaluate the performance by comparing it with the recent work in [31] and adjusting four parameters of the initial emotional state x_{p0}, x_{n0} λ_1, σ_1 and σ_2. Afterwards, we conduct the experiment to evaluate the performance of the prediction framework (PFDNN) which predicts the potential collective action based on deep neural network. The performance is measured with the precision, recall and F-measure. First, we conduct experiments to optimize the PFDNN by tweaking the parameters of the DNN. Second, to demonstrate the better performance of PFDNN, we compare it with the method called RF as proposed in [32] and the method called PFS as proposed in [15], all implemented by TensorFlow. Additionally, we analyze the performance of PFDNN in prediction of whether the potential collective action will occur every single day in the next 22 days, in order to compare with the performance of RF.

6.1 Datasets

To evaluate the performance of the two parts of the framework, we use two different datasets. Actually, the second part (DNN model) is the most important one and we need to compare the performance of the DNN model with other relevant research which uses the "Arab Spring" dataset. However, the "Arab Spring" dataset doesn't contain some key terms of the first part, such as the number of forwarded *user*'s posts, the number of *user*'s liked posts and the number of followers. Therefore, we have used two different datasets for evaluation purpose. For evaluating CECM, we implement experiments on six datasets about social events which are crawled from the Sina Microblog with the relation between users and keywords, including (1) Lasa, beating, smashing and looting; (2) Huan Yu, murder (a homicide case in 2016); (3) Fujian Bi (a TV host in CCTV); (4) Increase retirement age; (5) THAAD, Lotte; (6) online star, papi (the nickname of a female Internet celebrity). The six datasets are named as Dataset$i$ (i = 1,2,3,4,5,6) respectively. For each dataset, we approximately got 15,000 posts. After crawling the data, we can acquire the number of forwards and likes of all the posts for every user. As the list of key words of each social event we set is simple, some posts would be not very correlational. Taking into account the timeliness of news, the old posts are filtered based on the timestamp. For each record of the datasets there are 8 data items including:

user's ID, user's name, member or not, authentication or not, timestamp, forwarding times, commented times and liked times.

For evaluating PFDNN, the experiments are carried out based on 300,000 different open web content in Twitter collected by Recorded Future (*www.recordedfuture.com*). The dataset involves mass protests from 18 countries (for example Afghanistan, India, Egypt and Italy) which are about Arab Spring starting from Tunisia. As outlined above, we extract three features: the signal, violence-related words and emotion, from the tweets over a period of time. Then, we count the number of news published on mainstream media and make transformations to obtain Label $Y = 0$ or 1. Finally, we build the corresponding early premonitions using the features during k days, namely setting $k = 10$ for the certain Y. Thus, the inputs and outputs are produced to train the *DNN*.

6.2 Analysis of CECM

In this section we analyze the effect of the parameters including x_{p0}, x_{n0}, λ_i, σ_1 and σ_2 on the performance of CECM. Specifically: (1) we analyze how fast CECM can achieve the stable state during the dissemination process, which can be measured by the number of iterations (k) to achieve the stable solutions solved by the Runge-Kutta algorithm; (2) we try to verify the effect on theoretical equilibrium points in Table 1. In the experiment, the weights, α and β, are all set to be 0.5. That is, we believe the users' reliability and the development trend of the event have the same importance on the competitiveness. To conduct the experiments, we crawl all the $8.5521*10^7$ followers of 500 authenticated users from 50 industries and the average number is $1.7104*10^5$. Hence, λ_i was approximately set to be $1.7104*10^5$ when we analyze other parameters in the experiments.

First, the experiment analyzes the effect of λ_1 and λ_2 on the number of iterations and the final state. λ_1 and λ_2 are values from 100 to $1*10^6$ and $N_1 = 1.6*10^5$, $N_2 = 1*10^5$, $u = 0.03$, $\sigma_1 = 0.1, \sigma_2 = 0.8$, $x_{p0} = 0.1*10^5$, $x_{n0} = 0.15*10^5$. The results are presented in Table 2 and we can achieve several conclusions as follows.

1) For the number of iterations, it increases gradually with the growth of users' followers in group I_p while the number followers remaining unchanged in group I_n as shown in Experiment I and II in Table 2.
2) When λ_1 is set equal to λ_2, the number of iterations remains the same when λ_i is larger than a certain threshold value as shown in Experiment III in Table 2.
3) For the final states of x_p and x_n, there are extreme cases that x_p and x_n are very close to 0 and N_2 respectively when there is a big difference between λ_1 and λ_2 as shown in Experiment I in Table 2.
4) When λ_1 and λ_2 are equal and both larger than a certain threshold value, x_p and x_n finally approach to $1.5651*10^5$ and $0.2175*10^5$ respectively as shown in Experiment II and III in Table 2. But the threshold was not a fixed value and it depends on other parameters. Based on the experiments, the threshold is approximately 3000. We can see that λ_i has no effect on the number of iterations and the final state when λ_i is larger than the threshold value.

Next, the experiments evaluate the effect of σ_1 and σ_2 on the final values of x_p and x_n. Section VI has analyzed the theoretical effect of σ_i on the equilibrium points given the requirements of stability in Table 1. Hence in our experiments, we just need to choose one

Table 2 The effect of λ_i on the iteration and final state in different case

Experiment	λ_1	λ_2	Iteration	$x_p(*10^5)$	$x_n(*10^5)$
I	100	100	50	$0.345*10^{-5}$	$0.593*10^{-5}$
	100	1000	50	$0.002*10^{-3}$	$0.175*10^{-3}$
	100	10,000	50	0.00008	0.9989
	100	$1*10^5$	160	0.00004	0.9991
	100	$1*10^6$	259	0.00002	0.9999
II	10,000	10,000	50	1.5651	0.2175
	10,000	$1*10^5$	117	1.5649	0.2175
	10,000	$1*10^6$	761	1.5607	0.2195
III	2000	2000	50	$0.345*10^{-2}$	$0.593*10^{-2}$
	2500	2500	50	0.3452	0.5938
	3000	3000	72	1.5651	0.2175
	5000	5000	72	1.5651	0.2175
	10,000	10,000	72	1.5651	0.2175
	$1*10^5$	$1*10^5$	72	1.5651	0.2175
	$1*10^6$	$1*10^6$	72	1.5651	0.2175

pair of σ_1 and σ_2 for each requirement to analyze the variation. Based on Table 1, we consider three situations specifically: ① $0 < \sigma_1 < 1 - u < \sigma_2$; ② $\sigma_1 > 1 - u > \sigma_2 > 0$; ③ $0 < \sigma_1$, $\sigma_2 < 1 - u$ to analyze the variation of x_p and x_n. Compared with the situation where $\sigma_1 = \sigma_2 = 0$, the result indicates there is no interaction between group I_p and I_n. Note that here other parameters remain unchanged.

For situation ①, the experimental result is shown in Figure 5 where the solid line and the dotted line represent the variations of x_p and x_n respectively when $\sigma_1 = \sigma_2 = 0$, and the line marked with "*" and "O" represent the situation①. It shows that (x_p, x_n) is close to $(N_1, 0)$. The average accuracy is 97.172% compared with the theoretical equilibrium point $(N_1, 0)$.

For situation ②, the experimental result is shown in Figure 6. It shows that (x_p, x_n) is close to $(0, N_2)$. The average accuracy is 99.846% compared with the theoretical equilibrium point$(0, N_2)$.
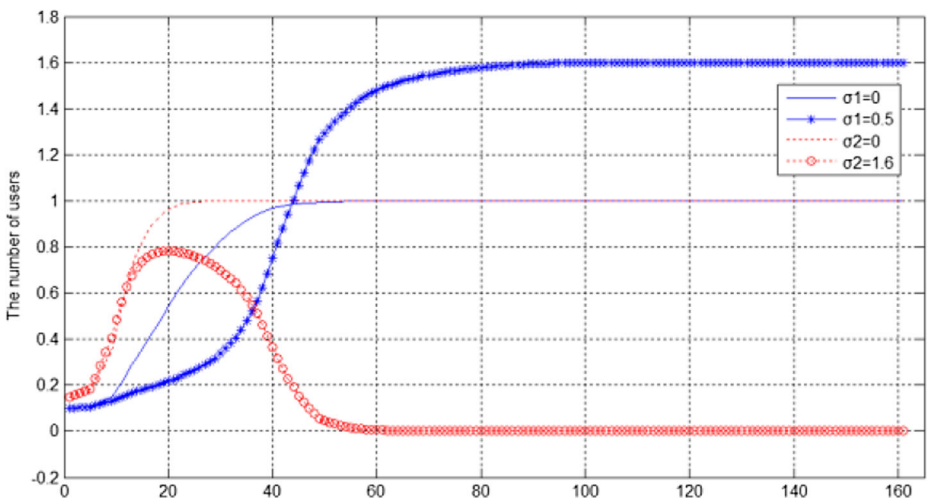
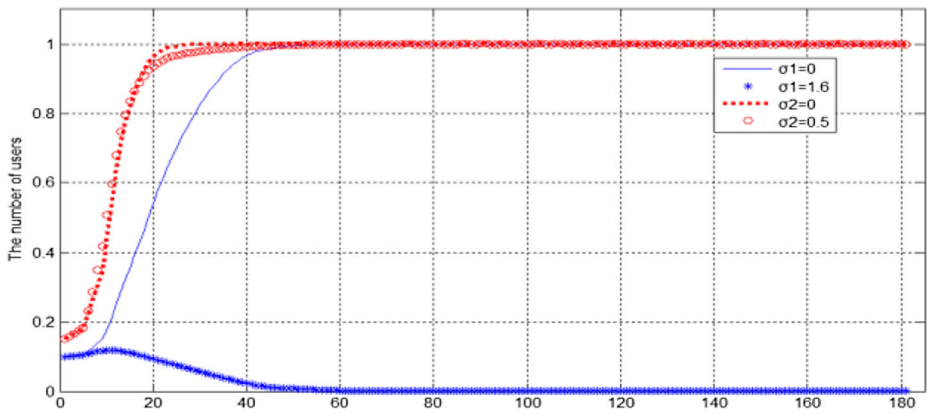**Figure 5** The effect of the situation ① on the x_p and x_n

Figure 6 The effect of the situation ② on the x_p and x_n

For situation ③, the experimental result is shown in Figure 7. It shows that (x_p, x_n) is close to $P_3(\frac{N_1(1-\sigma_1)(1-u)}{1-\sigma_1\sigma_2}, \frac{N_2(1-\sigma_2)(1-u)}{1-\sigma_1\sigma_2}) = (0.533*10^5, 0.833*10^5)$. The average accuracy is 99.846% compared with the theoretical equilibrium point $P_3(0.533*10^5, 0.833*10^5)$.

Finally, we try to verify whether the initial emotions can affect the final emotional state. The initial emotions fall into two categories, $x_{p0} > x_{n0}$ and $x_{p0} < x_{n0}$. Meanwhile, $N_1 = 1.6*10^5$, $N_2 = 1*10^5$, $\lambda_1 = 3000$, $\lambda_2 = 4000$, $u = 0.03$, $\sigma_1 = 0.5$, $\sigma_2 = 1.6$. The experimental result is shown in Table 3. We can see that no matter what the relation is between x_{p0} and x_{n0}, the result is always that x_p is close to N_1 and x_n is close to 0. Therefore, the final emotion state is not relying on the initial emotion.

In conclusion, if $0 < \sigma_1 < 1 - u < \sigma_2$, (x_p, x_n) moves towards to $P_1(N_1, 0)$. If $\sigma_1 > 1 - u > \sigma_2 > 0$, (x_p, x_n) moves towards to $P_2(0, N_2)$. If $1 - u > \sigma_1$, $\sigma_2 > 0$, (x_p, x_n) moves towards to $P_3(\frac{N_1(1-\sigma_1)(1-u)}{1-\sigma_1\sigma_2}, \frac{N_2(1-\sigma_2)(1-u)}{1-\sigma_1\sigma_2})$. And the other three parameters, viz. λ_1, λ_2 and u, can affect the speed of reaching to the stable state when they are lower than a certain threshold. However, there is no more effect when the values of these parameters exceed that threshold. Additionally,
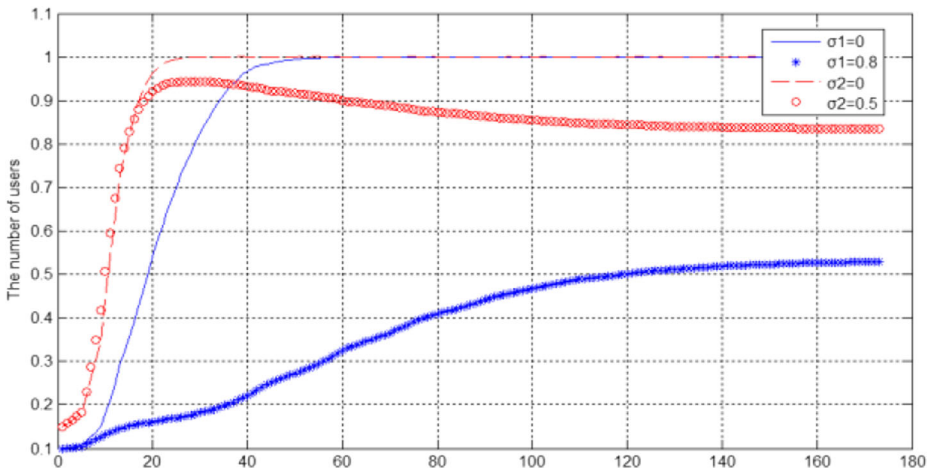

Figure 7 The effect of the situation ③ on the x_p and x_n

Table 3 The effect of initial emotions on the final state

$x_{n0}*10^5$	$x_{p0}*10^5$	x_p*10^5	x_n
0.15	0.1	1.6	0.00000057
0.35	0.3	1.6	0.00000031
0.15	0.2	1.6	0.00000095
0.45	0.4	1.6	0.00000014
0.57	0.5	1.6	0.00000005
0.25	0.5	1.6	0.00000021
0.35	0.5	1.6	0.00000011
0.45	0.6	1.6	0.00000023
0.57	0.6	1.6	0.00000004
0.57	0.7	1.6	0.00000005

it shows that the final emotional state does not depend on the initial emotion but significantly related to users' followers and the reliability of users' opinion.

6.2.1 Comparison of CECM with COCF

To further evaluate the performance of CECM, we compare it with the representative COCF model proposed in [31]. The proportions of the positive and negative posts each day on the Chinese microblog are different, which can reflect users' emotional state. We first obtain the number of users in the two emotion groups and then get the proportions. The performance is evaluated by the precision of the predicted proportions of the two emotions. COCF predicts the tendency and final emotional state of collective opinion by giving each user a conviction which measures the ability to insist on his/her opinion. It presents an opinion formation model via deduction, shown in Formula (15), in which users with high conviction are normally the opinion leaders. Note that there is a similarity between the conviction in COCF and the reliability measured by σ_1, σ_2 in *CECM*. Meanwhile, the result presented in [31] revealed that the final emotional state might deviate to either the positive or negative direction because of the initial bias of the leaders' opinions. O_s defined in Formula (20) reflects the probability of the two emotions which is similar to the proportions of the two emotions in *CECM*.

$$\begin{cases} O_s = \dfrac{r^2+r}{2r^2-r+1}^* \dfrac{1}{L} \sum_{i=1}^{L} o_i'(\text{s} = positive \quad or \quad negative) \\ \qquad\qquad r = \dfrac{L}{N} \end{cases} \tag{20}$$

where N is the number of users and o_i' is the opinion of the users whose conviction ranks at the i-th position in the system.

Here, we mainly compare the accuracy of CECM with that of COCF by analyzing the proportions of users who have either emotion in a stable state before the decay period. For COCF, the opinion leaders are identified by the number of followers which could be extracted from our real-world datasets. COCF depends on the first L leaders' emotions which are based on the ranking of the number of followers. In our experiment we set $L = N/3$ (N is the total number of users in the dataset, and the same with CECM). Leaders' emotions are reflected by their posts which could be checked manually or using textblob in Python. For CECM, the final state could be measured with equilibrium points, which has been proven to be more accurate in the experiments above.

For the six datasets, the final states of CECM and COCE are acquired. The accuracy is computed with Formula (21). As CECM depends on the current states, we chose different set of I_{p0} and I_{n0} with the $m = L = N/3$ (the same with COCF). In Formula (21), $y_{p,m}$ and $y_{n,m}$ represent the real stable ratios of I_p and I_n respectively, and I_{p0} and I_{n0} are both equal to m. Correspondingly, $\overline{y}_{p,m}$ and $\overline{y}_{n,m}$ are the predicted values. The results are shown in Table 4 and Table 5. We can find that the accuracy of CECM is higher than that of COCF in $Dataset_i$ ($i = 3,4,5,6$) and the average accuracy of CECM is also higher than that of COCF by 22.14%. Though the results in $Dataset_i$ ($i = 1,2$) show COCF is better than CECM, the gap is very small. The reason may be related to the characteristics of the datasets. So in general, we can conclude that the performance of CECM is better than that of COCF. We speculate the reason is that before social media becomes popular, COCF may have a better performance because the leaders' opinions are dominant and the information dissemination is not wide. However, with the rapid development of social media and its popularity among people, information dissemination becomes much wider so that much more people can discuss the event and make comments.

$$\text{Accuracy} = 1 - \frac{\left(|y_{p,m} - \overline{y}_{p,m}| + |y_{n,m} - \overline{y}_{n,m}|\right)}{2} \tag{21}$$

6.3 Analysis of PFDNN

The discriminator of PFDNN depends on DNN. We first select the activation function and the number of hidden layers based on the measurements of accuracy, precision, recall and F-measure by implementing many experiments on the dataset. Next, we compare DNN with two other research works on their average accuracy, precision, recall and F-measure. Finally, we further compare the performance of PFDNN with RF as proposed in [32] and PFS as proposed in [15] by analyzing the prediction accuracy for each day in the next 22 days.

6.4 Tweaking the parameters

As the outputs of the DNN in this research include two categories ($y_i = 0$ or 1), the output layer used "softmax" function is a two dimension vector of scores, one for each category. Meanwhile, the weights of each layer of the neural networks are initialized depending on the normal distribution and optimized with the Adam algorithm. For the DNN, the process of the experiments mainly consists of two steps: 1) selecting the suitable activation function, 2)

Table 4 The experiments on six real datasets extracted from the Chinese microblog for CECM

$Dataset_i$	σ_1	σ_2	$y_{p,m}$	$y_{n,m}$	$\overline{y}_{p,m}$(CECM)	$\overline{y}_{p,m}$(CECM)	Accuracy	Average Accuracy
1	$1.1761*10^{-4}$	0.0733	0.4189	0.5811	0.5190	0.4810	0.8454	0.8667
2	0.2470	0.1751	0.6622	0.3378	0.4772	0.5228	0.8151	
3	0.1383	0.3625	0.1757	0.8243	0.5748	0.4252	0.6009	
4	0.1582	0.2420	0.5000	0.5000	0.5262	0.4738	0.9738	
5	0.0544	0.0609	0.6622	0.3378	0.4983	0.4252	0.9932	
6	0.0185	0.3702	0.5811	0.4189	0.6091	0.3909	0.9720	

Table 5 The experiments on six real datasets extracted from the Chinese microblog for COCF

Data set$_i$	$y_{p,m}$	$y_{n,m}$	$\bar{y}_{p,m}$(COCF)	$\bar{y}_{p,m}$(COCF)	Accuracy	Average Accuracy
1	0.4189	0.5811	0.5555	0.4445	0.8634	0.7096
2	0.6622	0.3378	0.7897	0.2103	0.8724	
3	0.1757	0.8243	0.8012	0.1988	0.3745	
4	0.5000	0.5000	0.0237	0.9763	0.5237	
5	0.6622	0.3378	0.2236	0.7764	0.8047	
6	0.5811	0.4189	0.3998	0.6002	0.8187	

determining the number of the hidden layers and the number of nodes in each hidden layer (the node distribution).

For the activation functions, we consider six common functions (including relu, sigmoid, tanh, softplus, elu and relu6) and analyze their corresponding precision, recall and F-measure. When comparing their performance, the initial weights and the number of the layers are set as the same. We also analyze the impact on the performance by changing the numbers of the layers.

To select the best activation function, all other conditions are kept unchanged. The average results are shown in Table 6.

From Table 6, we can see that relu, softplus and elu function are the best choices in terms of recall, and the tanh function is the best one in terms of precision and F-measure. As F-measure is the comprehensive value of precision and recall, we regard tanh function as the best choice.

We also conduct experiments to analyze the performance of the DNN with different number of hidden layers ranging from 3 to 10 while keeping other conditions unchanged. To analyze the effect of the number of nodes, we increase the number of nodes gradually in a certain hidden layer while keeping others unchanged. By analyzing the experimental results, we can see the performance with 3 hidden layers is not desirable and it achieves the best performance when with the combination of [200, 20, 18] where 18 is the number of nodes in the final hidden layer. We adjust the number of nodes in each hidden layer, from 10 to 120 with an increment of 10. Eventually by analyzing the average performances and standard deviations of the accuracy, precision, recall and F-measure, we find that 9 hidden layers, namely 11 layers in total, might be most appropriate and there is no apparent difference with different number of nodes in the same hidden layers. The detailed experimental results are shown in Figures 8, 9, and 10.

In Figure 8, horizontal axis represented the total number of the hidden layers in the DNN. The vertical axis represented the average performances (the accuracy, the precision, the recall and the F-measure) when the DNN is structured with a certain number of hidden layers and the number of nodes ranging from 10 to 120. The result reveals that the performance is not desirable when the DNN is structured with 3, 4, or 5 hidden layers. The performance is improved with the increasing number of the hidden layers. As F-measure is the comprehensive

Table 6 The average results of six activation function in the DNN

Activation function	Precision	Recall	F-measure
Tanh	0.82	0.81	0.81
relu	0.5	1.0	0.67
Sigmoid	0.79	0.80	0.80
softplus	0.50	1.0	0.67
elu	0.50	1.0	0.67
Relu6	0.79	0.76	0.77
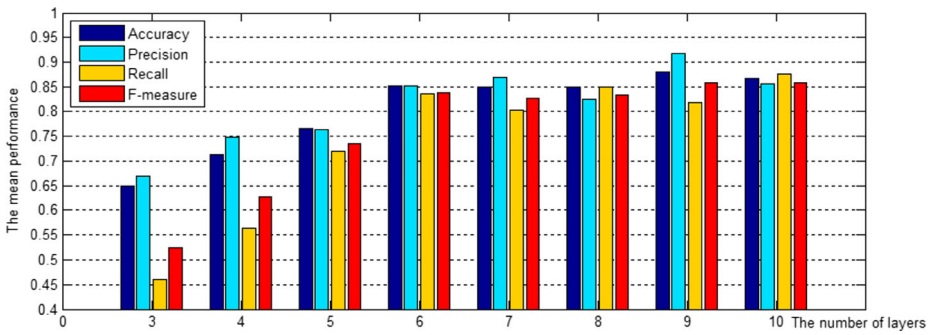
**Figure 8** The average performance of the DNN with different number of hidden layers

value of precision and recall, the accuracy and F-measure are considered as the two major evaluation metrics. Therefore, the DNN consisting of 9 hidden layers is regarded as the most appropriate one because it has the best accuracy and F-measure.

To evaluate the impact of different number of nodes, we adjust the number of nodes from 10 to 120 by an increment of 10 in the penultimate hidden layer when adding a new hidden layer, and keeping others unchanged. In the experiments, we obtain the four performance metrics illustrated in Figure 9. The corresponding standard deviations [33] calculated using Formula (22) which measure the discreteness of the datasets are illustrated in Figure 10.

$$\sigma = \sqrt{\frac{1}{N} \sum_{i=1}^{N} (x_i - \mu)^2} \qquad (22)$$

where μ denotes the mean of the dataset with components x_i and the number of the dataset is N.

Figure 9 shows the four performance metrics of the DNN with 9 hidden layers, and the results are mainly in the range from 0.8 to 0.95. Figure 10 shows the standard deviations of the four performance metrics, and the values are small when the number of the hidden layers is ranging from 6 to 10. Particularly, when the DNN was structured with 9 hidden layers, the standard deviations of all four metrics are the smallest in our experiments. Based on Figures 9 and 10, we
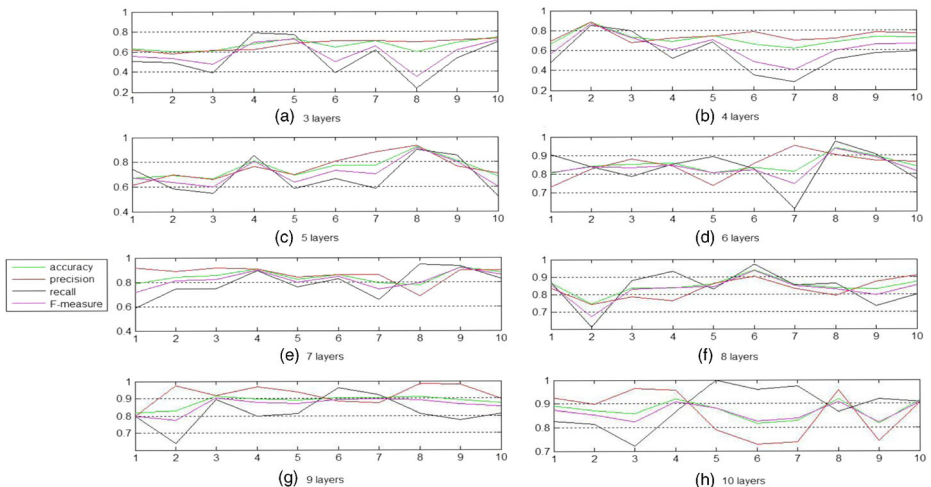
Figure 9 The performance with different number of nodes in the penultimate hidden layer in the DNN
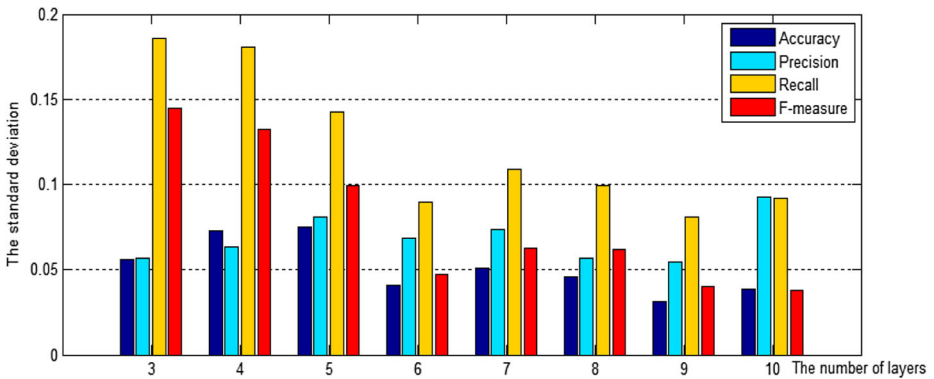
Figure 10 The standard deviations of the four performance metrics with different number of nodes in the penultimate hidden layer in the DNN

can see that the number of nodes has little effect on the performance of DNN in our experiments. For the DNN consisting of 11 layers with the following node distribution: [30, 200, 20, 20, 50, 80, 900, 60, 30, 18, 2], it is most stable as the four standard deviations were all the smallest and all the performance metrics are larger than 0.8.

To sum up, the relevant parameters of the DNN model were as follows: 1) The initial values of weights were based on normal distribution and the biases are initialized with 0.01. 2) The DNN model consisted of 11 layers with the following node distribution: [30, 200, 20, 20, 50, 80, 900, 60, 30, 18, 2]. 3) The activation function in each hidden layer used "tanh" function and the output layer uses "softmax" function. 4) The optimization objective of the DNN was based on the mean squared error and L2 regularization with the penalty term $\lambda=0.001$ the seen in formula (19). 5) The optimization objective was optimized with the Adam algorithm.

6.5 Comparison with other methods

The research in [32] proposed RF which is based on random forest and defined the collective action with two features: the number of tweets and the number of violence-related words. Additionally, RF employs the features during the last ten days to build the feature vector. The research in [15] proposed PFS which is a protest forecasting system that can identify what to look for using a combination of key phrase, reason about location occurrences in extracted results using probabilistic soft logic, and resolve future tense mentions using time normalization. The comparison depends on the performance metric of recall rate that indicates the maximum ability of identifying the collective actions. The experimental results are shown in Table 7. From the table, we can see that our PFDNN is better than RF and PFS as the average precision and recall are all higher than others.

Meanwhile, RF can also predict the collective actions for every single day in the next 22 days. For comparison purpose, we also implement that for PFDNN. The experimental results are shown in Figure 11. From the Figure, it shows that the performance of our research is better

Table 7 The comparison between PFDNN and RF, PFS

method	Average Precision	Average Recall
PFDNN	0.920	0.825
RF	0.658	0.755
PFS	0.710	0.510

than that of RF for predicting whether the collective action could occur in the next 22 days. It also shows that the accuracy would decrease gradually with the increase of the prediction period. Therefore, there might be merely a slight difference between a potential collective action and a regular activity at an early stage. However, they could show different early premonitions for the collective actions so that they could be detected by building early premonitions.

It should be noted that there are limitations to our predication framework. As the training set is built based on two kinds of data sources including the early premonitions collected from social media and the labels collected from mainstream media, the prediction framework cannot work if either kind of the data sources is not accessible. Besides, the two kinds of data sources need to contain time information because time correction is required for the early premonitions and the labels.

To guarantee the robustness of the DNN model in real-world applications, we apply multi-granularity testing criteria proposed in the work of [34] to evaluate the model. Based on these testing criteria, we can speculate that there may be some defects in the model when all input data are noises. However, this is only an extreme situation in reality. For most real-word applications, not all input data are noises and we can remove the noise data beforehand. Therefore, the impact of the defects can be reduced. Thus, it indicates that the robustness of the model is acceptable.

7 Related work

This study aims to predict the potential collective actions using emotional contagion and deep neural network. In this section, we will introduce related work on collective actions, emotional contagion and deep learning.

Study on Collective Actions Nathan Kallus [32] used random forest algorithm to determine whether an event can become a collective action based on the tweets and mainstream news on Arab Spring. This research analyzed collective actions by considering the amount of tweets and violence-related words in each tweet. Peng Lu studied on predicting the peak of people who participants in collective action [35]. Suhas Ranganath et al. studied how to predict
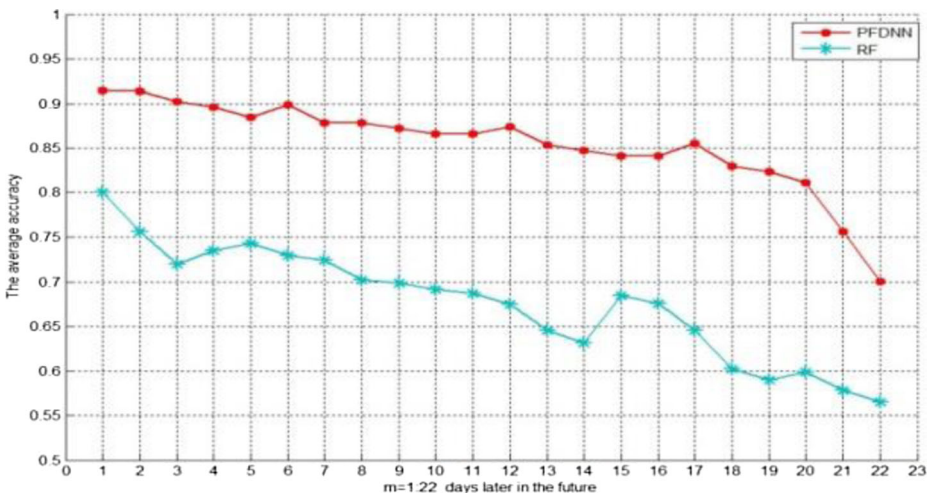
Figure 11 The accuracy of predicting collective actions every single day in the next 22 days

whether the user's next post would be a declaration of protest by analyzing his past status messages and the messages interacting with him over time [36]. Sandra González-Bailón et al. evaluated the theoretical claims about political protests by examining the cohesion of the networks using community detection methods [37]. Rupinder P. Khandpur et al. proposed an integrated situational assessment for airport related threats from news and social media to estimate if one airport is under higher threat than others [38]. Sathappan Muthiah et al. developed a protest forecasting system that can identify what to look for using a combination of key phrase, reason about location occurrences in extracted results using probabilistic soft logic, and resolve future tense mentions using time normalization [15].

Emotional contagion Collective emotions are at the heart of any society and become much more evident in gatherings, crowds, or responses to social events. As we know, negative emotions can easily result in demonstrations or even collective actions which can seriously affect the social security. Thus, the research on collective emotion is of great practical significance. Weibo (the Chinese microblog) generates more than 1000 posts every second. These posts not only convey facts, but also reflect the emotional states of the authors which can help understand user behaviors. The work in [39] built a system called MoodLens which is the first system developed for sentiment analysis of posts in Weibo. In MoodLens, 95 emoticons are mapped into the four categories of sentiments (including angry, disgusting, joyful, and sad) which serve as the class labels of posts. The authors in [40] proposed a theory that explains collective emotions from three broad perspectives: face-to-face encounters, shared culture and knowledge, and identification with a social collective. Furthermore, they stated that cognitive and affective states can be infectious under certain circumstances and spread through contagion. The work in [31] theoretically proposed a method for predicting the tendency and final state of collective opinion. The experiment showed that the collective opinion of the steady state may deviate to either the positive or negative direction based on the initial biases of the opinion leaders. The study further analyzed the correlation coefficient of the linear relationship between the collective opinion and the initial bias based on experimental as well as theoretical analysis. The authors in [41] proposed some interesting findings such as the phenomenon of emotion synchronization between friends in online social networks which reveals that emotion can be spread among users. Based on such findings, it presented a dynamic evolution model of collective emotions taking into account self-evolving as well as mutually evolving process. The study in [42] analyzed the dynamics of emotional contagion using Twitter. It showed that on average, a negative post has 4.34% more negative content than baseline, while positive posts has an average 4.50% more positive contents. Based on experimental evidence for massive-scale contagion via social networks, researchers also found that emotions expressed by others on Facebook influence our own emotions [43]. This work also suggested that, in contrast to prevailing assumptions, in-person interactions and nonverbal cues are not strictly necessary for emotional contagion, and that the observation of others' positive experience constitutes a positive experience for people.

Deep Learning Pascal Vincent et al. explored a straightforward variation on the stacking of ordinary autoencoders called denoising autoencoders which were trained locally to denoise corrupted versions of their inputs and could learn useful representations in a deep network [44]. Y LeCun et al. proposed LeNet-5 model which marked the formation of convolutional neural network [45]. Y LeCun, Yoshua Bengio and Geoffrey Hinton summarized the kernel knowledge of deep learning and explained the theory of CNN [46]. G. E. Hinton et al. proposed the method that it could train the neural network layer-by-layer to reduce the training complexity,

which gave a big push for the development of CNN and deep learning [47]. Alex Krizhevsky et al. used deep convolutional neural networks consisted of five convolutional layers (including max-pooling layers and two globally connected layers with a final 1000-way softmax) to study the classification problems on ImageNet [48]. In recent researches, face verification with CNN has been a very import domain. Sun Y et al. proposed to learn a set of high-level feature representations through deep convolutional networks (referred to as Deep hidden IDentity features (DeepID)) for multi-class face identification tasks [49]. In 2016, AlphaGo shocked the world by beating humans in playing the Game of Go. The research of AlphaGo also involved CNN which was introduced by D Silver et al. in the Nature Magazine [50].

8 Conclusions

Collective actions are usually planned, organized, and announced in advance and may threaten people's safety and the social stability. Therefore, it is very important to predict the occurrence and the date for collective actions in order to send out early warnings to decision-makers. For such a purpose, this paper proposed the prediction framework to predict whether a regular social activity can evolve into a collective action and estimate its date of occurrence using early premonitions. The framework is mainly comprised of two parts: the emotional contagion prediction and the DNN prediction. Emotional contagion prediction is used to forecast whether the whole emotional state will be negative or not. If not, we can conclude that the activity will not evolve into a collective action. Otherwise, we implement the DNN prediction framework. Our framework formulates the prediction problem as a binary classification problem where regular activity and collective action are the two output classes of the deep neural network. The framework can retrieve early premonitions from social media data and employ mainstream media data to label early premonitions during the training process of the DNN. Specifically, our experimental results showed that the DNN consisting of 11 layers with the node distribution [30, 200, 20, 20, 50, 80, 900, 60, 30, 18, 2] achieved the best performance.

Publisher's Note   Springer Nature remains neutral with regard to jurisdictional claims in published maps and institutional affiliations.

References

1. Siegel, D.A.: Social networks and collective action[J]. Am. J. Polit. Sci. **53**(1), 122–138 (2009)
2. Wu, L., Ge, Y., Liu, Q., et al.: Modeling the Evolution of Users' Preferences and Social Links in Social Networking Services[J]. IEEE Trans. Knowl. Data Eng. **29**(6), 1240–1253 (2017)
3. Hong, R., He, C., Ge, Y., et al.: User Vitality Ranking and Prediction in Social Networking Services: A Dynamic Network Perspective[J]. IEEE Trans. Knowl. Data Eng. **29**(6), 1343–1356 (2017)
4. Chen, Z., Tan, S.M., Campbell, R.H., et al.: Real Time Video and Audio in the World Wide Web[J]. World Wide Web J. (1995)

5. Nugroho, R., Zhao, W., Yang, J., et al.: Using time-sensitive interactions to improve topic derivation in twitter[J]. World Wide Web-internet. Web Inf. Syst. **20**(1), 61–87 (2017)
6. Xia, F., Yu, C., Xu, L., et al.: Top- k, temporal keyword search over social media data[J]. World Wide Web-internet. Web Inf. Syst. **20**(5), 1–21 (2017)
7. Hu, W., Wang, H., Qiu, Z., et al.: An event detection method for social networks based on hybrid link prediction and quantum swarm intelligent[J]. World Wide Web-internet. Web Inf. Syst. **20**(4), 1–21 (2017)
8. Fersini, E., Pozzi, F.A., Messina, E.: Approval network: a novel approach for sentiment analysis in social networks[J]. World Wide Web-internet. Web Inf. Syst. 1–24 (2016)
9. He, W.: Xu G. Social media analytics: unveiling the value, impact and implications of social media analytics for the management and use of online information[J]. Online Inf. Rev. **40**(1), 369–370 (2016)
10. Chinchore, A., Jiang, F., Xu, G.: Intelligent Sybil Attack Detection on Abnormal Connectivity Behavior in Mobile Social Networks[C]//International Conference on Knowledge Management in Organizations, pp. 602–617. Springer, Cham (2015)
11. eMarketer. eMarketer Releases Latest Estimates for Worldwide Messaging App Usage[EB/OL]. https://www.emarketer.com/Article/eMarketer-Releases-Latest-Estimates-Worldwide-Messaging-App-Usage/1016214. 21 July 2017
12. Tufekci, Z., Wilson, C.: Social media and the decision to participate in political protest: Observations from Tahrir Square[J]. J. Commun. **62**(2), 363–379 (2012)
13. Cihon, P., Yasseri, T.A.: Biased Review of Biases in Twitter Studies on Political Collective Action[J]. Front. Phys. **4**(6), 91 (2016)
14. Schneider, N.: Occupy Wall Street[J]. Nation. **29**, (2011)
15. Muthiah, S., Huang, B., Arredondo, J., et al.: Planned Protest Modeling in News and Social Media[C]// AAAI, pp. 3920–3927. (2015)
16. Chen, E., Zeng, G., Luo, P., et al.: Discerning individual interests and shared interests for social user profiling[J]. World Wide Web-internet. Web Inf. Syst. **20**(2), 417–435 (2017)
17. Xu, G., Li, L., Zhang, Y., et al.: Modeling user hidden navigational behavior for Web recommendation[J]. Web Intelligence Agent Syst. **9**(3), 239–255 (2011)
18. Dos Santos, C.N., Gatti, M.: Deep Convolutional Neural Networks for Emotion Analysis of Short Texts[C]// COLING, pp. 69–78. (2014)
19. Krizhevsky, A., Sutskever, I., Hinton, G.E.: Imagenet classification with deep convolutional neural networks[C]//Advances in neural information processing systems, pp. 1097–1105. (2012)
20. Kim, Y.: Convolutional neural networks for sentence classification[C], pp. 1746–1751. arXiv preprint arXiv (2014)
21. Deng, S., Huang, L., Xu, G., et al.: On Deep Learning for Trust-Aware Recommendations in Social Networks.[J]. IEEE Trans. Neural Netw. Learn Syst. **28**(5), 1164 (2017)
22. Davydov, A.A., Platov, A.S.: Optimal stationary solution in forest management model by accounting intra-species competition[J]. Moscow Math. J. **12**(2), 269–273 (2012)
23. Eckersten, H., Lundkvist, A., Torssell, B., et al.: Modelling species competition in mixtures of perennial sow-thistle and spring barley based on shoot radiation use efficiency[J]. Acta Agric. Scand. Sect. B Soil Plant Sci. **61**(8), 739–746 (2011)
24. Sharma, S., Samanta, G.P.: Optimal harvesting of a two species competition model with imprecise biological parameters[J]. Nonlinear Dyn. **77**(4), 1101–1119 (2014)
25. Foster, K.R., Bell, T.: Competition, not cooperation, dominates interactions among culturable microbial species[J]. Curr. Biol. **22**(19), 1845–1850 (2012)
26. Lou, Y., Munther, D.: Dynamics of a three species competition model[J]. Discrete Contin. Dynam. Systems. **32**(9), 3099–3131 (2012)
27. Mirrahimi, S., Perthame, B., Wakano, J.Y.: Evolution of species trait through resource competition[J]. J. Math. Biol. **64**(7), 1189–1223 (2012)
28. Tran, M.V., O'Grady, M., Colborn, J., et al.: Aggression and Food Resource Competition between Sympatric Hermit Crab Species[J]. PLoS One. **9**(3), e91823–e91823 (2014)
29. Allesina, S., Levine, J.M.: A competitive network theory of species diversity[J]. Proc. Natl. Acad. Sci. **108**(14), 5638–5642 (2011)
30. Torices, R., Méndez, M.: Fruit size decline from the margin to the center of capitula is the result of resource competition and architectural constraints[J]. Oecologia. **164**(4), 949–958 (2010)
31. Hou, L., Liu, J., Pan, X., et al.: Prediction of collective opinion in consensus formation[J]. Int. J. Mod. Phys. C. **25**(4), 222–237 (2014)
32. Kallus, N.: Predicting crowd behavior with big public data[C]// Pro-ceedings of the companion publication of the 23rd international con-ference on World wide web companion, pp. 625–630. International World Wide Web Conferences Steering Committee (2014)
33. Bland, J.M., Altman, D.G.: Statistics notes: measurement error[J]. BMJ. **313**(7059), 744 (1996)

34. Ma, L., Juefei-Xu, F., Sun, J., et al.: DeepGauge: Comprehensive and Multi-Granularity Testing Criteria for Gauging the Robustness of Deep Learning Systems[J]. arXiv preprint arXiv:1803.07519 (2018)
35. Lu, P.: Predicting peak of participants in collective action[J]. Appl. Math. Comput. **274**, 318–330 (2016)
36. Ranganath, S., Morstatter, F., Hu, X., et al.: Predicting Online Protest Participation of Social Media Users[C]//AAAI, pp. 208–214. (2016)
37. González-Bailón, S., Borge-Holthoefer, J., Rivero, A., et al.: The dynamics of protest recruitment through an online network[J]. Sci. Rep. **1**, 197 (2011)
38. Khandpur, R.P., Ji, T., Ning, Y., et al.: Determining Relative Airport Threats from News and Social Media[C]//AAAI, pp. 4701–4707. (2017)
39. Zhao, J., Dong, L., Wu, J., et al.: MoodLens: an emoticon-based sentiment analysis system for Chinese tweets[C]// ACM SIGKDD International Conference on Knowledge Discovery and Data Mining, pp. 1528–1531. ACM (2012)
40. Scheve, C.V., Ismer, S.: Towards a Theory of Collective Emotions[J]. Emot. Rev. **5**(4), 406–413 (2013)
41. Xiong, X.B., Zhou, G., Huang, Y.Z., et al.: Dynamic evolution of collective emotions in social networks: a case study of Sina weibo[J]. SCIENCE CHINA Inf. Sci. **56**(7), 1–18 (2013)
42. Ferrara, E., Yang, Z.: Measuring Emotional Contagion in Social Media.[J]. PLoS One. **10**(11), (2014)
43. Kramer, A.D.I., Guillory, J.E., Hancock, J.T.: Experimental evidence of massive-scale emotional contagion through social networks[J]. Proc. Natl. Acad. Sci. **111**(24), 8788–8790 (2014)
44. Vincent, P., Larochelle, H., Lajoie, I., et al.: Stacked denoising autoencoders: Learning useful representations in a deep network with a local denoising criterion[J]. J. Mach. Learn. Res. **11**(12), 3371–3408 (2010)
45. LeCun, Y., Bottou, L., Bengio, Y., et al.: Gradient-based learning applied to document recognition[J]. Proc. IEEE. **86**(11), 2278–2324 (1998)
46. Lecun, Y., Bengio, Y., Hinton, G.: Deep learning[J]. Nature. **521**(7553), 436–444 (2015)
47. Hinton, G.E., Salakhutdinov, R.R.: Reducing the dimensionality of data with neural networks[J]. Science. **313**(5786), 504–507 (2006)
48. Krizhevsky, A., Sutskever, I., Hinton, G.E.: Imagenet classification with deep convolutional neural networks[C]//Advances in neural information processing systems, pp. 1097–1105. (2012)
49. Sun, Y., Wang, X., Tang, X.: Deep Learning Face Representation from Predicting 10,000 Classes[C]// IEEE Conference on Computer Vision and Pattern Recognition, pp. 1891–1898. IEEE Computer Society (2014)
50. Silver, D., Huang, A., Maddison, C.J., et al.: Mastering the game of Go with deep neural networks and tree search[J]. Nature. **529**(7587), 484 (2016)

Affiliations

Wei Yang [1] · Xiao Liu [2] · Jin Liu [3,4,5] · Xiaohui Cui [1]

Wei Yang
yangweisklse@whu.edu.cn

Xiao Liu
xiao.liu@deakin.edu.au

Jin Liu
jinliu@whu.edu.cn

[1]   School of Cyber Science and Engineering, Wuhan University, Wuhan 430072, China

[2]   School of Information Technology, Deakin University, Melbourne 3125, Australia

[3]   State Key Laboratory of Software Engineering, Computer School, Wuhan University, Wuhan 430072, China

[4]   Guangxi Key Laboratory of Trusted Software, Guilin University of Electronic Technoloy, Guilin 541004, China

[5]   Key Laboratory of Network Assessment Technology, Institute Of Information Engineering, Chinese Academy Of Sciences, Beijing 100093, China